NJC

Accepted Manuscript

This is an *Accepted Manuscript*, which has been through the Royal Society of Chemistry peer review process and has been accepted for publication.

Accepted Manuscripts are published online shortly after acceptance, before technical editing, formatting and proof reading. Using this free service, authors can make their results available to the community, in citable form, before we publish the edited article. We will replace this *Accepted Manuscript* with the edited and formatted *Advance Article* as soon as it is available.

You can find more information about *Accepted Manuscripts* in the Information for Authors.

Please note that technical editing may introduce minor changes to the text and/or graphics, which may alter content. The journal's standard Terms & Conditions and the Ethical guidelines still apply. In no event shall the Royal Society of Chemistry be held responsible for any errors or omissions in this *Accepted Manuscript* or any consequences arising from the use of any information it contains.

ROYAL SOCIETY OF CHEMISTRY

www.rsc.org/njc

Highly Sensitive p-Nitrophenol Chemical Sensor Based on Well-Crystalline α-MnO_2 Nanotubes

Jingwen Wu[1], Qiang Wang [1,*], Ahmad Umar[2,3]*, Shihao Sun[1], Liang Huang[1], Junya Wang[1], Yanshan Gao[1]

[1]College of Environmental Science and Engineering, Beijing Forestry University, 35 Qinghua East Road, Haidian District, Beijing 100083, P. R. China

[2]Department of Chemistry, College of Science and Arts, Najran University, Najran-11001, Kingdom of Saudi Arabia

[3]Promising Centre for Sensors and Electronic Devices (PCSED), Najran University, Najran-11001, Kingdom of Saudi Arabia

***Corresponding authors:**

Professor Qiang Wang:

E-mail address: qiang.wang.ox@gmail.com; qiangwang@bjfu.edu.cn

Tel: +86 13699130626

Professor Ahmad Umar:

E-mail address: ahmadumar786@gmail.com,

Tel: +966-534574597

Table of content (TOC)

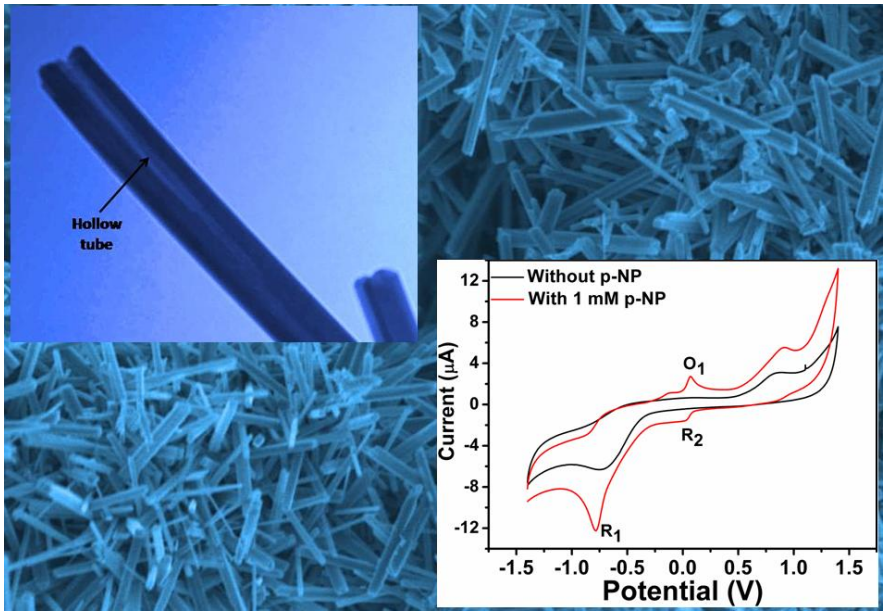

Well-crystalline α-MnO_2 nanotubes were synthesized and used as potential scaffold for the efficient detection of p-nitrophenol chemical

Abstract

This paper reports the successful fabrication and characterization of highly sensitive p-nitrophenol (p-NP) amperometric chemical sensor based on well-crystalline α-MnO_2 nanotubes. The α-MnO_2 nanotubes were successfully synthesized using a simple hydrothermal treatment of potassium permanganate ($KMnO_4$) and concentrated hydrochloric acid (HCl). The prepared nanotubes were examined in detail by using various analytical methods which revealed that the synthesized nanotubes are grown in very high density, possessing well-crystallinity and purity. The as-synthesized α-MnO_2 nanotubes were used for the fabrication of p-NP chemical sensor which exhibited high sensitivity of 19.18 $mA \cdot mM^{-1} \cdot cm^{-2}$ and low detection limit of 0.1 mM. To best of our knowledge, this is the first report that used α-MnO_2 nanotubes to fabricate p-NP chemical sensor with such high sensitivity and low detection limit.

Keywords: α-MnO_2 nanotubes; 4-Nitrophenol chemical sensor; nanomaterials; phenolic compounds

1. Introduction

Phenolic compounds are protoplasmic poisons that have a toxic effect on humans, animals and plants. They are extensively used in the production of dyes, pharmaceuticals, pesticides, insecticides and so on [1, 2]. Overexposure to these compounds by inhalation, ingestion, eyes or skin contacts can result in comas, convulsions, cyanosis, and even death for the human beings [3]. Phenolic compounds, especially p-nitrophenol (p-NP) are considered as priority pollutants because they are harmful to living organisms even at low concentrations. p-NP is an intermediate or a final product in the degradation pathway of organo-phosphorous pesticides and has huge impact on humans owing to their persistence and toxicity. Furthermore, it is highly soluble in water and is found in both terrestrial and aquatic environment. This hazardous substance can result in physical, chemical and biological changes in water, and consequently have a negative impact on human health[4-6]. Due to the highly hazardous nature of p-NP towards human beings and animals, it is important to manufacture an efficient, reliable, robust and highly sensitive chemical sensor for the detection of p-NP.

Various methods such as fluorescence[7], capillary, electrophoresis [8], gas chromatography [9, 10], high performance liquid chromatography [11], and liquid chromatography combined with mass spectrometry [12], etc have been reported in the literature which are widely used to investigate even low-concentration of hazardous chemicals. However, these methods require a complicated, time-consuming sample treatment process, and also cause damage to the expensive instruments [1], which is not

economical for large-scale use in industry and daily life. Among various techniques, the electrochemical method is regarded as a promising approach for the determination of p-NP with portability, cost effectiveness, high sensitivity and reliability [13, 14]. The performance of electrochemical process strongly depends on the electrode material [15-17]. However, one disadvantage of electrochemical methods is that the over-potential is high and the detection selectivity is poor, if a conventional electrode is used as an electrochemical detector or transducer [18]. As a result, much effort has been devoted in developing advanced materials that have outstanding electrochemical properties to modify commercial electrodes.

In recent years, different metal oxides have attracted great attention for the fabrication of electrochemical sensors in the fields of environmental analysis. There are some reports on the detection of p-NP using, Mg(Ni)FeO [19], metal oxide-composite nanoparticles [20], reduced graphene oxide/Au nanoparticle composite [21], and CuO nanotubes [13]. Among theses nanostructured metal oxides, manganese dioxides (MnO_2) have drawn particular attention owing to their low cost, high activity, and non-toxicity [22]. MnO_2 can form different types of polymorphs including α-, β-, γ-, and δ-, which leads to distinctive properties and wide applications like molecular sieves, ion sieves, catalysts, cathode materials of secondary rechargeable batteries, and new magnetic materials [23]. Even though MnO_2 have been applied in a variety of applications, to the best of our knowledge, there is no literature available for the application of α-MnO_2 nanomaterial to the sensoring of p-NP. Thus in this contribution, we have synthesized high quality well-crystalline α-MnO_2 nanotubes

using a simple hydrothermal method and utilize the prepared nanotubes to fabricate p-NP chemical sensor with high sensitivity (19.18 $mA \cdot mM^{-1} \cdot cm^{-2}$) and low-detection limit of 0.1 mM. The prepared α-MnO_2 nanotubes were also characterized in detail in terms of their morphological, structural and compositional properties.

2. Experimental details

2.1 Synthesis of α-MnO_2 nanotubes

The potassium permanganate ($KMnO_4$) and concentrated hydrochloric acid (HCl) utilized in the synthesis of α-MnO_2 were purchase from Bejing Chemical Works, and used without any further purification. In a typical experimental procedure, 2.5 mmol $KMnO_4$ and 10 mmol HCl were added to 45 mL de-ionized water (DW). The obtained precursor solution was then transferred into a Teflon-lined stainless steel autoclave with a capacity of 65 mL, which was sealed and hydrothermally treated at 140 ^oC for 12h. After completing the reaction, the autoclave was cooled down to room-temperature naturally and finally black precipitates were collected by centrifugation and washed several times by DW and dried in air overnight [24].

2.2 Characterization of α-MnO_2 nanotubes

The as-synthesized α-MnO_2 nanotubes were characterized in details by different techniques. The morphologies of the nanotubes were investigated by field emission scanning electron microscopy (FESEM) and transmission electron microscopy (TEM). The crystallinity and crystal phases were examined by the X-ray diffraction (XRD,

Shimadzu XRD-6000) pattern measured with Cu-Kα Radiation in the range of 10^{o}–70^{o} at a scanning rate of 5^{o} /min. The chemical composition of as-synthesized α-MnO_2 nanotubes were examined by Fourier transform infrared (FT-IR) spectroscopy, measured at room temperature, in the range of 400–4000 cm^{-1}.

2.3 Fabrication and characterization of p-NP sensor based on α-MnO_2 nanotubes

Before modification, the surface of glassy carbon electrode (GCE) was polished with 1.0, 0.3, and 0.05 μm alumina slurry for ten minutes respectively, followed by rinsing with DW thoroughly and then dried at room temperature. The α-MnO_2 nanotubes modified GCE was prepared as follows: 5.0 mg α-MnO_2 nanotube powder were dispersed in 1.0 mL water and ultrosonicated for 30 min, then 5 μL of the suspension was dropped on the freshly cleaned GCE surface (surface area: 0.0707 cm^2) and dried in ambient conditions for 3h. Electrochemical experiments were conducted on a CHI 660D electrochemical workstation (Shanghai Chenhua Company, China). All the electrochemical experiments were performed at room temperature with a three electrode system in which the modified GCE was used as working electrode, a Pt wire as a counter electrode and a saturated calomel electrode as reference. For all the measurements, 0.1 M phosphate buffer solution (PBS; PH=7.0) was used.

3. Results and discussion

3.1 Structural and morphological properties of as-synthesized α-MnO_2 nanotubes

To examine the structural, crystallinity and crystal phases, the as-prepared material was examined by X-ray diffraction (XRD) at room-temperature with Cu-Kα Radiation in the range of 10^{o}–70^{o} at a scanning rate of 5^{o}/min. For XRD analysis, the prepared α-MnO_2 powder was used. Figure 1 exhibits the typical XRD pattern of as-prepared powder which exhibited several well-defined diffraction reflections. Interestingly, it was confirmed from JCPDS data card no. 44-0141, that all the observed diffraction reflections are well-matched with well-crystalline α-MnO_2. The observed well-defined diffraction reflections appeared at 12.6, 18.1, 25.5, 28.6, 36.6, 37.5, 38.7, 41.1, 41.8, 46.1, 47.3, 49.8, 56.3, 60.1, 65.2, 66.9, and 69.3° are assigned as MnO_2 (110), (200), (220), (310), (400), (211), (330), (420), (301), (321), (510), (411), (600), (521), (002), (112), and (541), respectively. The observed diffraction reflections are sharp and intense and no other reflections were observed in the pattern which indicated that the synthesized α-MnO_2 nanomaterials are well-crystalline without any significant impurity up to the detection limit of X-ray.

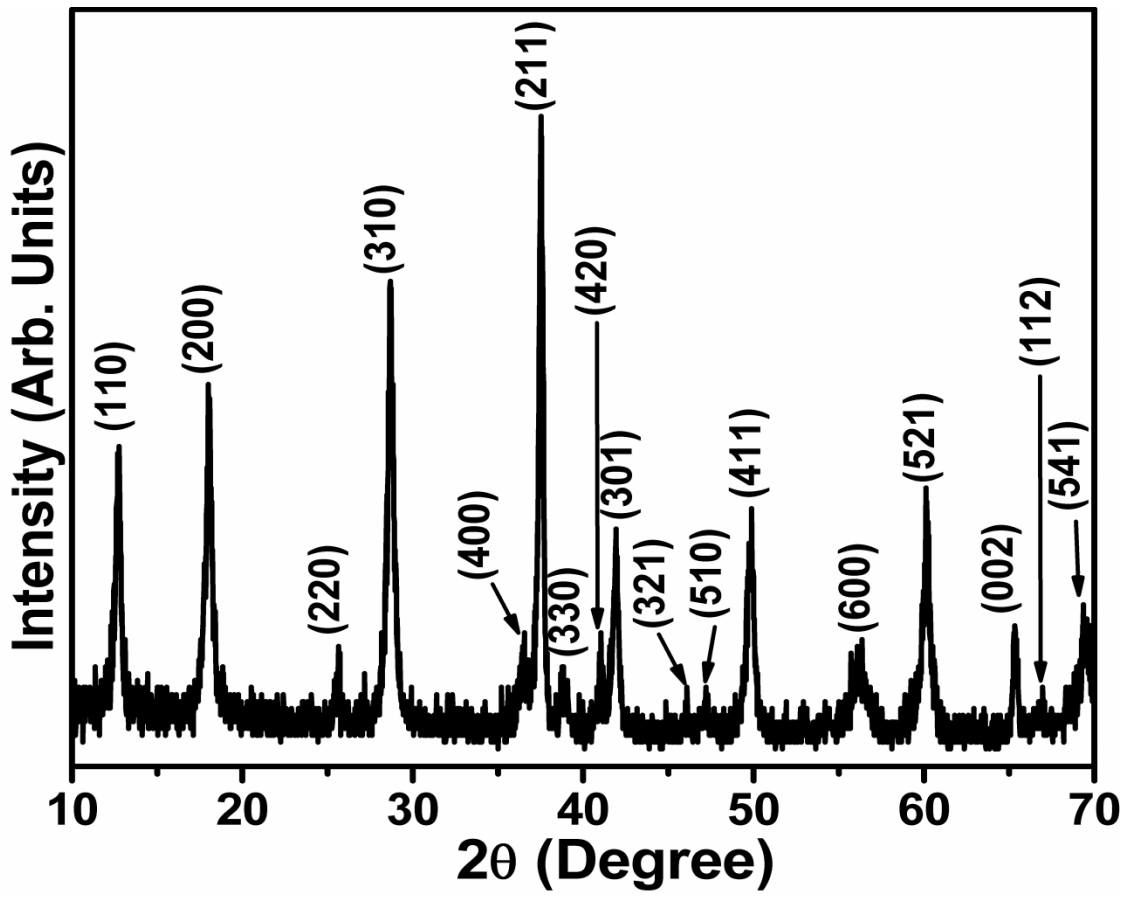

Figure 1. Typical XRD pattern of as-synthesized α-MnO_2 nanotubes

The general morphologies of as-prepared α-MnO_2 material were examined by FESEM and TEM. Figure 2 (a) and (b) exhibited typical FESEM images which revealed that the prepared materials are nanotubes which are synthesized in very high density. Figure 2 (c) and (d) exhibited high-resolution FESEM images of as-synthesized α-MnO_2 nanotubes. The nanotubes exhibited tetragonal shapes with hollow interiors. The diameters of the nanotubes are not uniform and vary from 55 nm to 90 nm. The typical lengths of the prepared nanotubes are in the range of 2-3 μm. The nanotubes exhibited smooth and clean surfaces throughout their lengths.

For further and detailed morphological characterizations, the prepared α-MnO_2

nanotubes were examined by TEM. For TEM observations the as-prepared α-MnO_2 nanotubes were ultrasonically dispersed in Acetone and a drop of acetone solution which contains the α-MnO_2 nanotubes was placed on a copper grid and examined. Figure 3 (a) and (b) exhibit the typical TEM image of as-synthesized α-MnO_2 nanotubes. The observed TEM images are well consistent with the FESEM results in terms of their morphologies and dimensionalities. The observed TEM images confirmed that the prepared α-MnO_2 nanotubes possess smooth and clean surfaces throughout their length with well-defined hollow interiors. The typical diameters of the nanotubes are in the range of 70 ± 20 nm. To examine the crystallinity and crystal quality, the prepared nanotubes were further characterized by selected area electron diffraction (SAED) pattern attached with TEM (inset 3 (b)). The selected area electron diffraction pattern reveals a well defined, ordered diffraction pattern indicating well-crystallinity for the prepared α-MnO_2 nanotubes.

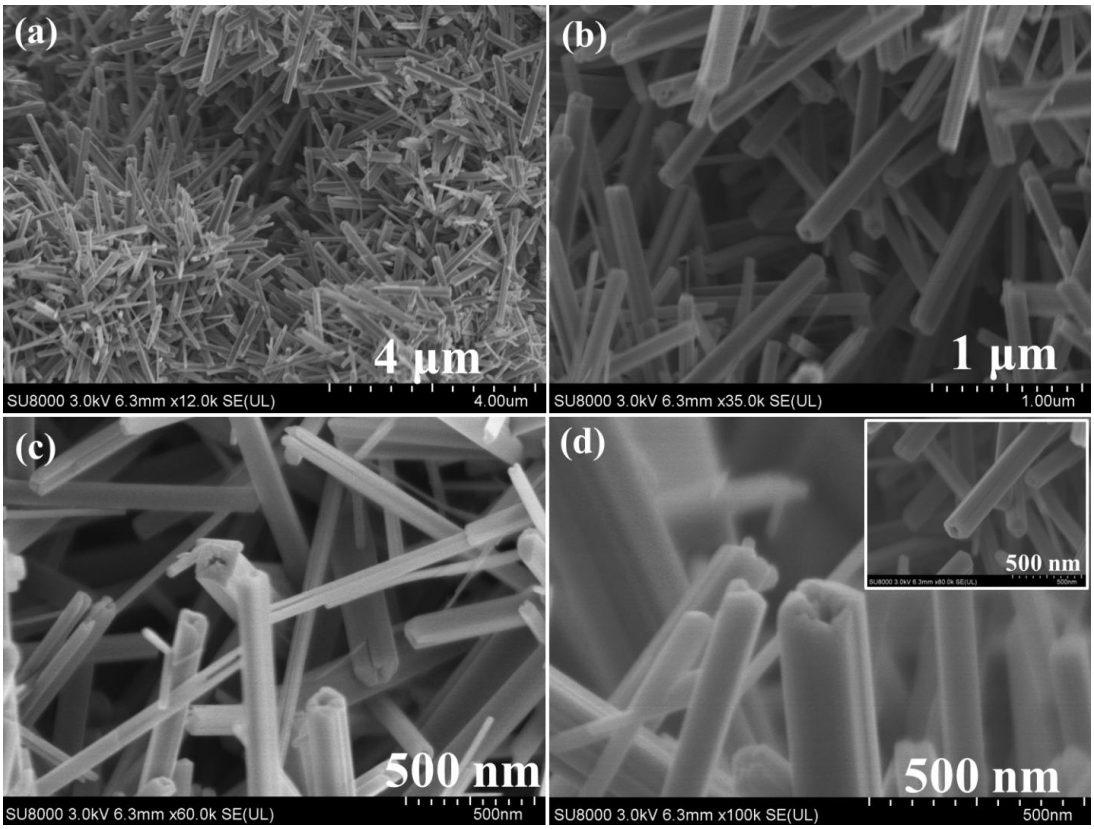

Figure 2. Typical FESEM images of as-synthesized α-MnO_2 nanotubes

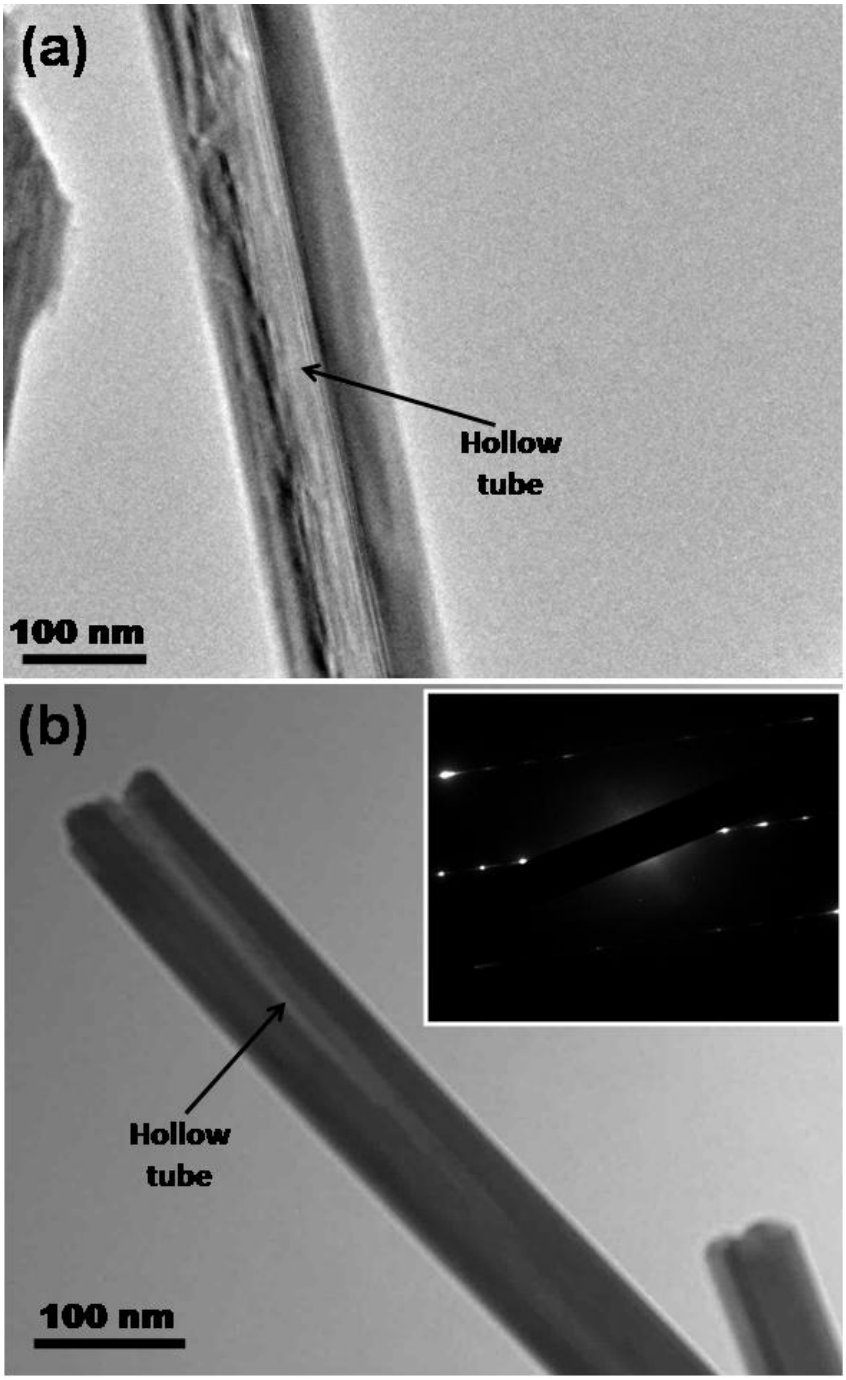

Figure 3. Typical (a) and (b) TEM images of as-synthesized α-MnO_2 nanotubes. Inset (b) shows the SAED pattern of corresponding α-MnO_2 nanotube.

To examine the chemical compositions and purity, the as-synthesized α-MnO_2 nanotubes were characterized by FTIR spectroscopy measured at room temperature, in the range of 400–4000 cm^{-1}. To measure FTIR of as-prepared sample, certain

amount of as-synthesized α-MnO_2 nanotubes was mixed well with potassium bromide (KBr) and compressed under high-pressure of ~4 tons to form the pellet. The prepared pellet was then used for the FTIR measurement. Figure 4 exhibits the typical FTIR spectrum of as-synthesized α-MnO_2 nanotubes. Several well-defined peaks are seen in the observed FTIR spectrum at 437, 527, 712, 1631 and 3421 cm^{-1}. The observed broadband appeared at 3421 cm^{-1} for α-MnO_2 nanotubes can be assigned to the absorbent of interlayer hydrates and some hydroxyl groups not from the hydrates but those directly bound to the metal ions. The bands appeared at 1631 cm^{-1} represents the vibrations from the interaction of Mn with surrounding species such as OH, O, H^+ and K^+ [25,26]. Basu et al. also reported that the hydrous α-MnO_2 samples also show a peak at 1620 cm^{-1} [27]. Finally, the absorption peaks at 712 cm^{-1}, 527 cm^{-1} and 473 cm^{-1} revealed the Mn-O vibrations from MnO_6 octahedra, which confirms the formation of α-MnO_2 nanocrystals [25, 28, 29].

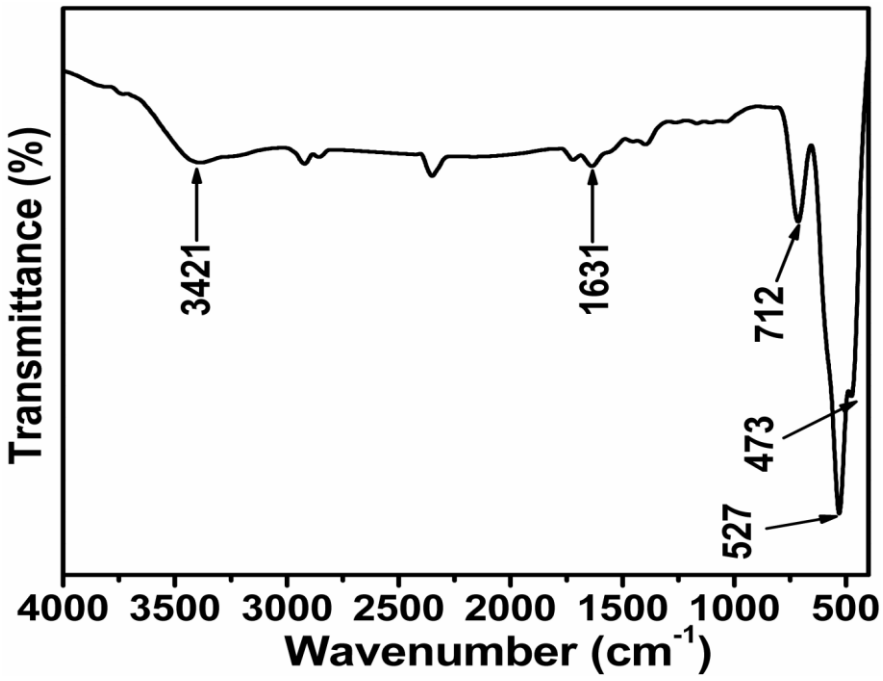

Figure 4. Typical FTIR spectrum of as-synthesized α-MnO_2 nanotubes

3.2 Electrochemical p-NP sensor performance of α-MnO_2 nanotubes modified GC Electrodes

To fabricate the p-NP amperometric chemical sensor, the as-prepared α-MnO_2 nanotubes were deposited on GC electrode. The p-NP amperometric chemical sensor performance was evaluated by three electrode system in which the α-MnO_2 nanotubes modified electrode was used as working electrode, a Pt wire as a counter electrode and a saturated calomel electrode as reference electrode.

Figure 5 exhibited the representative CV graph of α-MnO_2 nanotubes modified GCE in the absence (black line) and presence (red line) of p-NP in 0.1 M PBS at scan rate of 50 mV/s. It is apparent from the observed CV analysis that when a small amount of p-NP (1 mM) was added in the PBS solution, the CV graph exhibited a clear irreversible reduction peak (R_1) appears at around -0.78 V with the current of Ip = -12.26 μA. Also a pair of reversible peak O_1 and R_2 appeared at around 0.070 V (Ip= 2.714 μA) and 0.0162 V (Ip= -1.594 μA), respectively. This phenomenon confirmed that the as-prepared α-MnO_2 nanotubes are promising candidate for the efficient detection of p-NP.

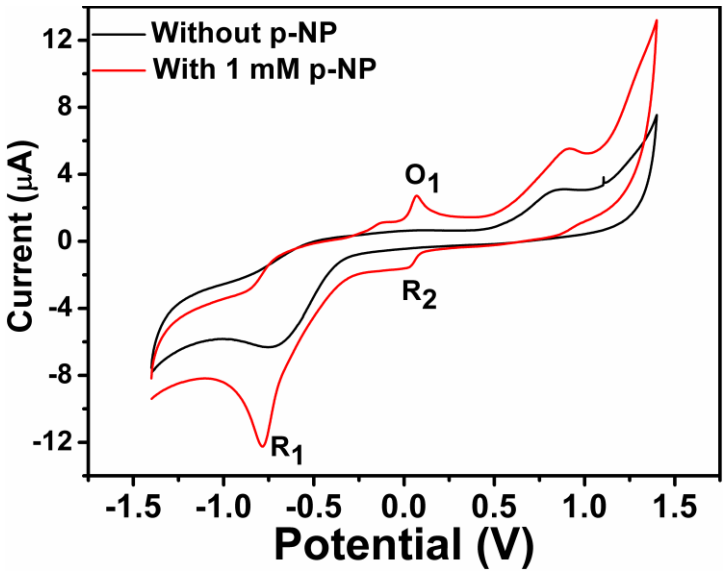

Figure 5. Typical CV sweep curve for α-MnO_2 nanotubes modified electrode without (black line) and with 1 mM p-NP (red line) at a scan rate of 50 mV/s in 10 mL PBS.

The effect of scan rates on the performance of α-MnO_2 modified GCE was also conducted by cyclic voltammetry in a wide range of scan rates from 50 mV/s to 900 mV/s in 0.1 M PBS containing 1 mM p-NP. Figure 6 shows the CV response of the modified electrode at scan rates of 50, 60, 70, 80, 90, 100, 200, 300, 400, 500, 600, 700, 800 and 900 mV/s. Interestingly, it was observed that all the *Ip* values of oxidation and reduction peaks increased with the increase of scan rates, and exhibited a linear relation to the square root of the scan rate (Figure 6 (b)), indicating that diffusion process controls the kinetics of the overall process[14, 30].

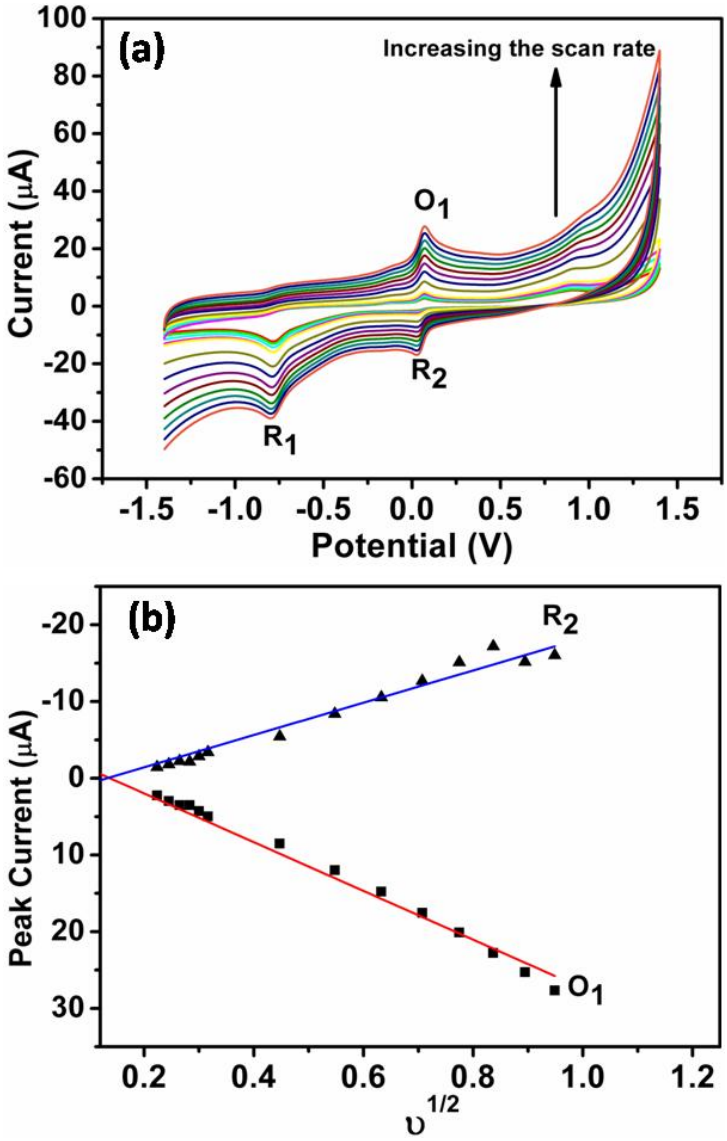

Figure 6. (a) CV sweep curves at different scan rates (50, 60, 70, 80, 90, 100, 200, 300, 400, 500, 600, 700, 800 and 900 mV/s) and (b) anodic peak current vs. square root of scan rate ($v^{1/2}$).

To examine in detail the sensing performance of the fabricated p-NP chemical sensor, a series of CV measurements were performed with α-MnO_2 nanotubes modified electrode using different concentrations (from 0.1 mM to 1 mM) of p-NP in 0.1 M PBS at 50 mV/s. Figure 7 (a) shows a series of CV measurements at several

p-NP concentrations from 0.1 mM to 1 mM of the fabricated α-MnO_2 nanotubes modified electrode.

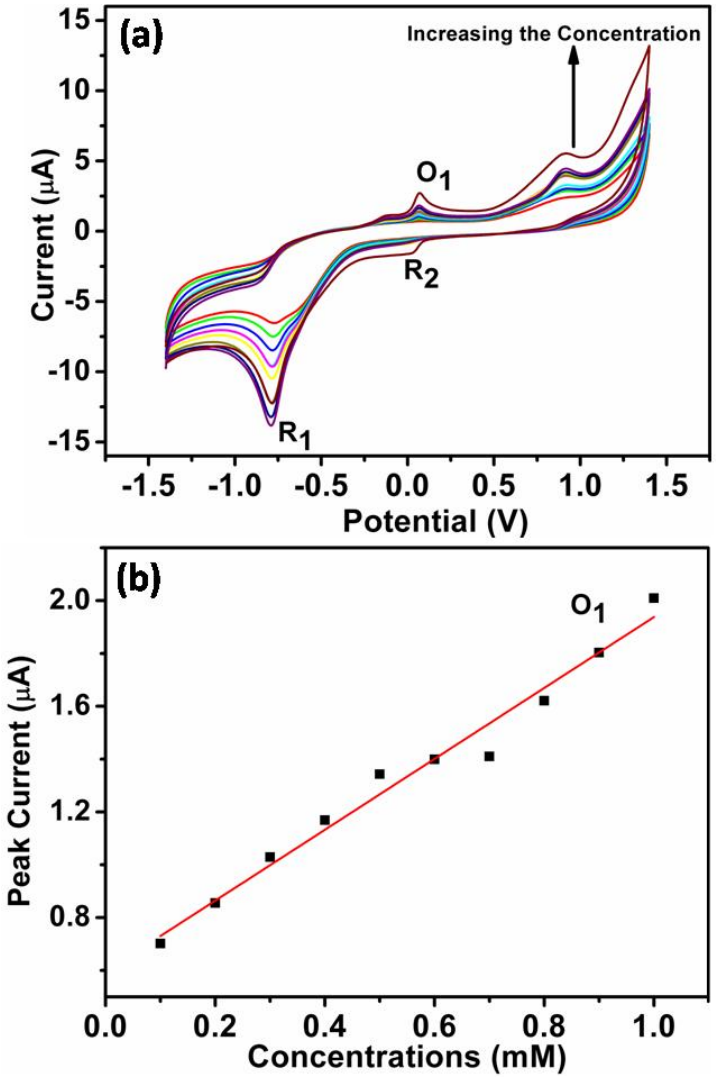

Figure 7. (a) CV response of α-MnO_2 nanotubes modified electrode with different concentrations of p-NP from 0.1 mM to 1 mM at 50 mV/s and (b) anodic peak current vs. concentrations of p-NP.

From the observed results, it is seen that with increasing the concentrations of p-NP, the peak currents (O_1) also increases. Moreover, the peak potential also shifted

positively. It was interesting to observe that by adding the p-NP into PBS solution, an increase in the current response was observed which revealed that the α-MnO_2 nanotubes modified electrode has sensitive a rapid response towards p-NP. This fast electrical response of the modified electrode can be related with the fast redox reaction and good electro-catalytic oxidation properties of the fabricated α-MnO_2 nanotubes based sensors and p-NP.[30-32] Figure 7 (b) demonstrates the typical graph for the anodic peak current vs. concentrations of p-NP which demonstrates that the oxidation current increases linearly with the p-NP concentration (n=10, R=0.9763).

Scheme 1 depicts the typical and proposed electrochemical reaction mechanism of p-NP on α-MnO_2 nanotubes modified electrode[33]. During the reaction, at the initial step, the p-nitroso-phenol undergoes redox reaction and produce p-hydroxyl-amino-phenol. During the reaction, later the oxidation of p-hydroxyl-amino-phenol takes place which give rise to 4-nitrosophenol and the subsequent reversible reduction. In the CV measurement, the large reduction peak shows the reduction of p-NP to 4-hydroxy-amino-phenol (figure 5) while the pair of coupled redox peaks indicate the oxidation of 4-hydroxy-amino-phenol to 4-nitrosophenol and the subsequent reversible reduction.

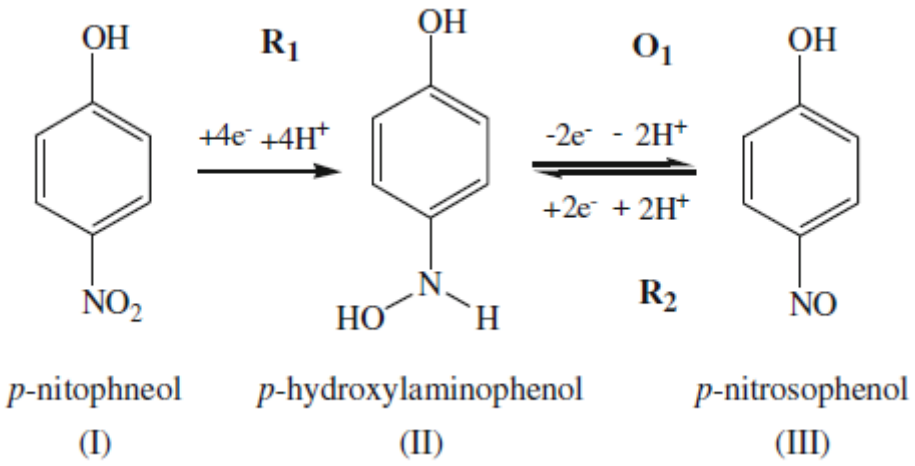

Scheme 1. Electrochemical reaction mechanism of p-NP on α-MnO_2 nanotubes modified electrode

The amperometric experiments were also performed and the constant potential was set at 0.95 V for the experiment with successive addition of p-NP from 0.1 mM to 0.7 mM into continuously stirred 0.1 M PBS solution of PH=7.0. As can be seen in Figure 8(a), a rapid increase in the current was observed after each addition of p-NP into the electrolyte solution. The response current increases with increasing the concentration of p-NP, and exhibited a liner relationship between current *vs*. p-NP concentrations with a correlation coefficient of 0.9841 (Figure 8 (b), n=7). The detection limit for the fabricated p-NP chemical sensor was found to be 0.1 mM (S/N=3). The sensitivity was determined by the slope of the calibration curve and the area of the electrode was calculated by the following equation: πR2, where R is measured to be 0.15 mm. Therefore, the sensitivity, calculated from slope of calibration curve/area of electrode, was found to be 19.18 $mA \cdot mM^{-1} \cdot cm^{-2}$. To evaluate the performance of α-MnO_2 nanotubes modified electrode, previously

reported p-NP chemical sensors fabricated based on different mediators were compared and shown in Table 1. The observed sensitivity for the fabricated p-NP chemical sensor is very much higher than the other reported p-NP electrochemical sensor fabricated based on the utilization of various material electron mediators such as ordered mesoporous carbons/GCE[34], Mg(Ni)FeO/CPE[19] , molecularly imprinting chitosan/phenyltrimethoxysilane/AuNPs hybrid film[35], graphene/polymer/GCE[1], Mn_2O_3-ZnO nanoparticles/flat-silver electrodes[20], reduced graphene oxide/Au nanoparticle composite/GCE[21], CuO nanotubes/GCE[13], etc. Moreover, in terms of the detection limit, the α-MnO_2 nanotubes modified electrode exhibited smaller detection limit than that of graphene/polymer composites based electrode[1]. The fabricated p-NP chemical sensor shows very good reproducibility and it was found that the fabricated sensor did not show any significant decrease in the sensitivity for more than 3 weeks, while storing in an appropriate form when not in use. Finally, from the observed results, it is clear that the α-MnO_2 nanotubes are promising material for the effective determination of p-NP.

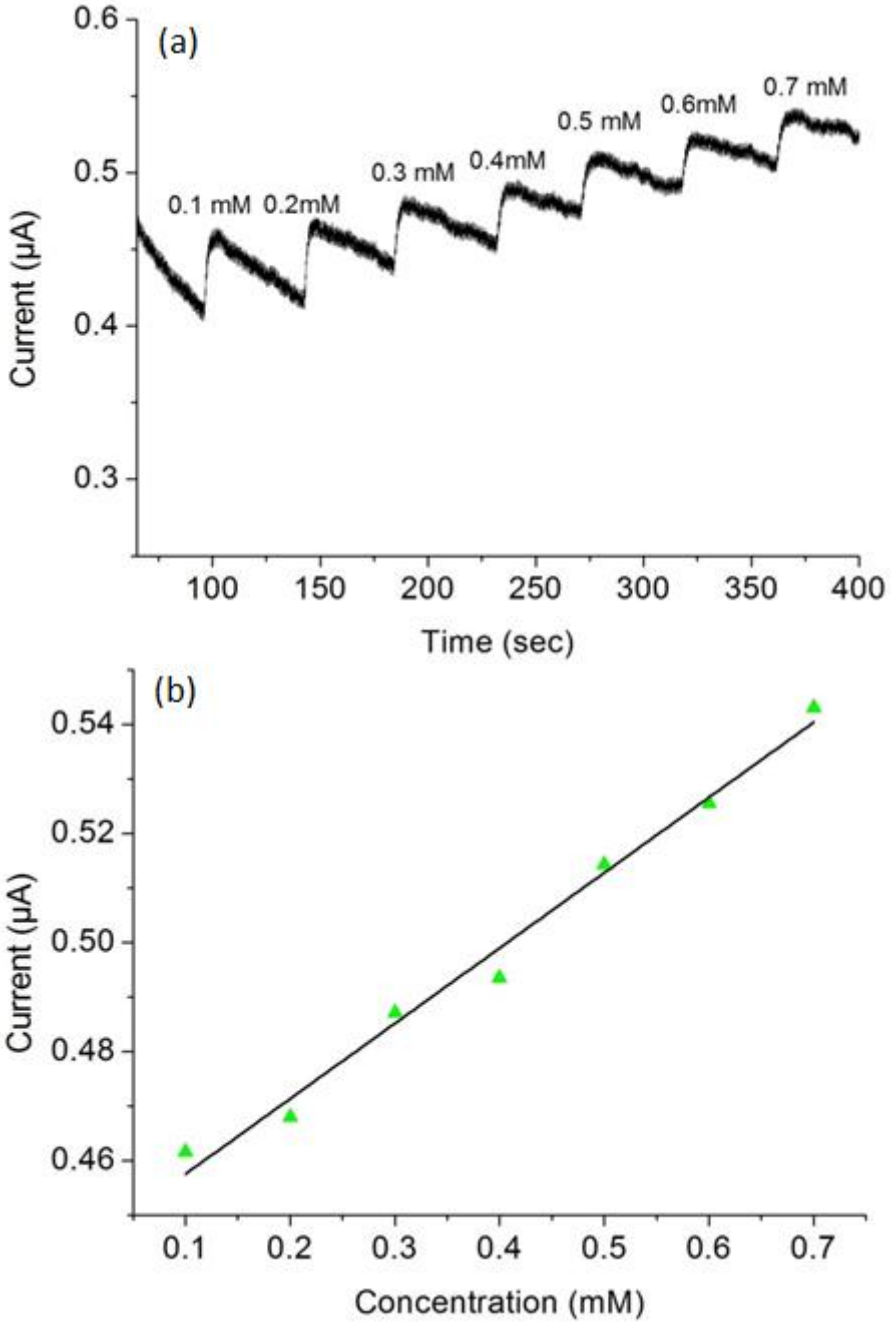

Figure 8. (a) Amperometric response of the α-MnO_2 nanotubes modified electrode with successive addition of p-NP into 0.1 M PBS solution and (b) current vs. concentrations of p-NP.

Table 1. Comparison summary of the performances of p-NP chemical sensors fabricated based on different nanomaterials modified electrode.

Electrode materials	Sensitivity ($mA \cdot mM^{-1} \cdot cm^{-2}$)	Detection limit	Linear range	Ref.
α-MnO_2 nanotubes/GCE	19.18	0.1 mM	0.1 mM -0.7 mM	This work
Ordered mesoporous carbons /GCE	-	0.1 μM	2 μM-90 μM	32
Mg(Ni)FeO/CPE	0.811	0.2 μM	2.0 μM-200 μM	19
Molecularly imprinting chitosan/phenyltrimethoxy silane/AuNPs hybrid film	-	5.0 nM	30.0 nM-35.0 mM	33
Graphene/polymer/GCE	-	20.0 mM	5.331μM-0.4887 mM	1
Mn_2O_3-ZnO nanoparticles/flat-silver electrodes	~4.6667	~0.83 ± 0.2 nM	0.1 nM-50.0 μM	20
Reduced graphene oxide/Au nanoparticle composite/GCE	-	0.01 μM	0.05-2.0μM	21
CuO nanotubes/GCE	~0.13284±0.02	~5 nM	10 nM-1 mM	13

4. Conclusion

In conclusion, well-crystalline α-MnO_2 nanotubes were synthesized using a simple hydrothermal treatment and were characterized by different techniques to investigate its morphological and structural properties. Moreover, the as-synthesized α-MnO_2 nanotubes were utilized as an efficient electron mediator for the fabrication of p-NP chemical sensor. The modified sensor based on α-MnO_2 nanotubes exhibited

reliable high sensitivity of 19.18 $mA \cdot mM^{-1} \cdot cm^{-2}$ and low-detection limit of 0.1 mM. The obtained linear range for the fabricated sensor was from 0.1 mM to 0.7 mM. The presented work demonstrates that α-MnO_2 nanomaterials can efficiently be used for the fabrication of highly sensitive and reproducible chemical sensor.

Acknowledgements

This work is supported by the Fundamental Research Funds for the Central Universities (TD-JC-2013-3), the Beijing Nova Programme (Z131109000413013), the Program for New Century Excellent Talents in University (NCET-12-0787), the National Natural Science Foundation of China (51308045), the Key Laboratory of Functional Inorganic Material Chemistry (Heilongjiang University). Ahmad Umar would like to acknowledge the Ministry of Higher Education, Kingdom of Saudi Arabia for the research grant (PCSED-001-11) under the Promising Centre for Sensors and Electronic Devices (PCSED) at Najran University.

References

1. (a) K. Chen, Z. Zhang, Y. Liang and W. Liu, Sensors, 2013, **13**, 6204; (b) C. Chen, Hangrong Chen, Jianlin Shi, and Jianchang Yu, Sci. Adv. Mater. 2013, **5**, 896
2. (a) A. Niaz, J. Fischer, J. Barek, B. Yosypchuk, N. C. Sirajuddin and M. I. Bhanger, Electroanalysis, 2009, **21**, 1786.; (b) Daimei Chen, Yanxi Deng, Qian Zhu, Gaoxiang Du, and Fengsan Zhou, Sci. Adv. Mater. 2013, **5**, 1041;
3. R. Arasteh, M. Masoumi, A. Rashidi, L. Moradi, V. Samimi and S. Mostafavi, Appl. Surf. Sci. , 2010, **256**, 4447.
4. (a) P. Patnaik and J. Khoury, Water Res., 2004, **38**, 206; (b) Hava Ozay, Sci. Adv. Mater. 2013, **5**, 575
5. (a) F. C. Moraes, S. T. Tanimoto, G. R. Salazar-Banda, S. A. S. Machado and L. H. Mascaro, Electroanalysis, 2009, **21**, 1091; (b) D. P. Mohapatra, S. K. Brar, P. Picard, and R. D. Tyagi, Sci. Adv. Mater. 2013, **5**, 57
6. B. R. Zaidi and S. H. Imam, J.Gen. Appl. Microbiol., 1996, **42**, 249.
7. W. Zhang, C. R. Wilson and N. D. Danielson, Talanta, 2008, **74**, 1400.
8. X. Guo, Z. Wang and S. Zhou, Talanta, 2004, **64**, 135.
9. S. Wang and H. Chen, J. Chromatogr. A, 2002, **979**, 439.
10. J. A. Padilla-Sánchez, P. Plaza-Bolaños, R. Romero-González, A. Garrido-Frenich and J. L. M. Vidal, J. Chromatogr. A, 2010, **1271**, 5724.
11. D. Hofmann, F. Hartmann and H. Herrmann, Anal. Bioanal. Chem., 2008, **391**, 161.
12. R. Wissiack and E. Rosenberg, J. Chromatogr. A 2002, **963**, 149.
13. M. Abaker, G. N. Dar, A. Umar, S. A. Zaidi, A. A. Ibrahim, S. Baskoutas and A. Al-Hajry, Sci. Adv. Mater., 2012, **4**, 893.
14. S. K. Mehta, K. Singh, A. Umar, G. R. Chaudhary and S. Singh, Electrochim. Acta, 2012, **69**, 128.
15. R. Kötz, S. Stucki and B. Carcer, J. Appl. Electrochem., 1991, **21**, 14.
16. Y. Xu, Y. Wang, Y. Ding, L. Luo, X. Liu and Y. Zhang, J. Appl. Electrochem.,

2013, **43**, 679.

17. B. J. Sanghavi and A. K. Srivastava, Analyst, 2013, **138**, 1395.
18. D. Zhao, X. Zhang, L. Feng, L. Jia and S. Wang, Colloids Surf., B: Biointerfaces, 2009, **74**, 317.
19. Y. Xu, Y. Wang, Y. Ding, L. Luo, X. Liu and Y. Zhang, J. Appl. Electrochem. , 2013, **43**, 679.
20. (a) M. Rahman, G. Gruner, M. S. Al-Ghamdi, M. A. Daous, S. B. Khan and A. M. Asiri, Chem. Central J. , 2013, **7**, 60; (b) Haroldo G. Oliveira, Bob C. Fitzmorris, Claudia Longo, and Jin Z. Zhang, Sci. Adv. Mater. 2012, **4**, 673
21. Y. Tang, R. Huang, C. Liu, S. Yang, Z. Lu and S. Luo, Anal. Methods, 2013, **5**, 5508.
22. (a) A. Wang, P. Zhang, Y. Li, J. Feng, W. Dong and X. Liu, Microchim Acta, 2011, **175**, 31; (b) Devaraj Soundararajan, Yong Il Kim, Jong-Huy Kim, Ki Hyeon Kim, and Jang Myoun Ko, Sci. Adv. Mater. 2012, **4**, 805
23. B. Tang, G. Wang, L. Zhuo and J. Ge, Nanotechnology, 2006, **17**, 947.
24. J. Luo, H. Zhu, H. Fan, J. Liang, H. Shi, G. Rao, J. Li, Z. Du and Z. Shen, J. Phys. Chem. C, 2008, **112**, 12594.
25. Y. Li, J. Wang, Y. Zhang, M. N. Banis, J. Liu, D. Geng, R. Li and X. Sun, J. Colloid Interface Sci., 2012, **369**, 123.
26. C. M. Julien, M. Massot and C. Poinsignon, Spectrochim. Acta, Part A : Mol. Biomol. Spectrosc., 2004, **60**, 689.
27. S. Dutta, J. K. Basu and R. N. Ghar, Sep. Purif. Technol. , 2001, **27**, 227.
28. T. Gao, H. Fjellvåg and P. Norby, Anal. Chim. Acta, 2009, **648**, 235.
29. S. Gnanam and V. Rajendran, J. Alloys Compd., 2013, **550**, 463.
30. Y. Bai, Y. Du, J. Xu and H. Chen, Electrochem Commun, 2007, **9**, 2611.
31. R. S. Nicholson and I. Shain, Anal. Chem., 1964, **36**, 706.
32. R. C. Reid, J. M. Prausnitz and B. E. Poling, The properties of gases and liquids, McGraw-Hill, New York, 1987.
33. F. C. Moraes, S. T. Tanimoto, G. R. Salazar-Banda, S. A. S. Machado and L. H.

Mascaro, Electroanalysis, 2009, **21**, 1091.

34. T. Zhang, Q. Lang, D. Yang, L. Li, L. Zeng, C. Zheng, T. Li, M. Wei and A. Liu, Electrochimica Acta, 2013, **106**, 127.

35. S. Li, D. Du, J. Huang, H. Tu, Y. Yang and A. Zhang, Analyst, 2013, **138**, 2761.